

EFFECT OF FERRITE PHASE ON THE FORMATION AND COEXISTENCE OF $3\text{CaO}\cdot 3\text{Al}_2\text{O}_3\cdot \text{CaSO}_4$ AND $3\text{CaO}\cdot \text{SiO}_2$ MINERALS

XIAOLEI LU^{*, **}, CHUANHAI LI^{*, **}, SHUXIAN WANG^{*}, #ZHENGMAO YE^{*, **}, #XIN CHENG^{*, **}

^{*}School of Materials Science and Engineering, University of Jinan,
Jinan, Shandong 250022, China

^{**}Shandong Provincial Key Laboratory of Preparation and Measurement of Building Materials,
Jinan, Shandong 250022, China

[#]E-mail: mse_yezm@163.com (Zhengmao Ye), mse_chengxin@163.com (Xin Cheng)

Submitted August 10, 2017; accepted October 20, 2017

Keywords: Ferrite, $3\text{CaO}\cdot 3\text{Al}_2\text{O}_3\cdot \text{CaSO}_4$, $3\text{CaO}\cdot \text{SiO}_2$, Coexistence

The effect of ferrite on the formation and coexistence of $3\text{CaO}\cdot 3\text{Al}_2\text{O}_3\cdot \text{CaSO}_4$ ($C_4A_3\$$) and $3\text{CaO}\cdot \text{SiO}_2$ (C_3S) was investigated in this paper. The results indicate that 20 % content of ferrite phase with the composition of $C_2A_{0.5}F_{0.5}$ can facilitate the coexistence of $C_4A_3\$$ and C_3S solid solutions at 1350°C. There are other trace elements that incorporate into clinker minerals and form solid solutions. In addition, the dark and polygonal $C_4A_3\$$ solid solution is not dissolved in liquid phase at 1350°C. It can promote the burnability of the raw mixes and provide a favorable condition for the formation of C_3S . However, it has an adverse effect on the coexistence of two clinker minerals with the changing of ferrite compositions. This will provide the important basis for the preparation of the calcium sulphoaluminate cement clinker containing C_3S .

INTRODUCTION

Ye'elimit (C₄A₃§) and alite (C₃S) are the most important cementitious minerals of calcium sulphoaluminate cement (CSA) and Portland cement (PC) respectively. CSA has the high early strength, small volume shrinkage during hydration and corrosion resistance [1-3]. However, the mechanical strength of mortar shows a slow increase owing to the low reactivity of C₂S at medium hydration ages (between 7 d and 28 d). C₃S is responsible for early and medium mechanical strengths in PC. Hence, a possible approach is to bring in C₃S minerals in the production of the CSA clinker. Consequently, it is necessary to solve this issue that make the two minerals (C₄A₃§ and C₃S) coexist with the clinker.

Extensive researches on the formation and coexistence of C₄A₃§ and C₃S minerals with doping minor elements has been carried out, which could lower the viscosity and the formation temperature of liquid phase, and promote the formation of C₃S. I. Odler [4, 5] investigated the SO₃-rich Portland clinkers containing simultaneously the phases C₄A₃§ and C₃S, which was prepared by burning pertinent raw meals with adding small amounts of CaF₂ at 1300°C. Liu and Li [6, 7] produced the clinker at temperatures between 1250°C and 1300°C by adding CaF₂ and MgO as mineralizers. Ma [8] reported the mineral formation and coexistence of C₄A₃§ and C₃S in the clinker could be achieved by adding CuO and CaF₂. In addition to using the mineralizer,

Shen [9, 10] prepared alite-ye'elimit cement clinker by a secondary heat treatment step at 1250°C after regular Portland clinker firing at 1450°C. In current researches, adding the CaF₂ mineralizer is the main way to achieve the coexistence of C₄A₃§ and C₃S in the production of clinker [11-13]. No doubt that CaF₂ could contribute more to the formation of C₃S at lower temperatures by lowering its free energy relative to C₂S [14]. However, CaF₂ has its own drawbacks, for instance, environment pollution owing to fluoride ion, corrosion of the refractory materials in cement kiln, and low the hydraulic activity of cement [15, 16], which is restricted in the industrial applications.

The composition and content of liquid phase have the significant influence on the C₃S formation in the production of clinker. The liquid phase are mainly composed of CaO, Al₂O₃ and Fe₂O₃ in burning process. The viscosity of liquid phase varies with the ionic state in the liquid composition. CaO is always dissociated into Ca²⁺ ions, while Al₂O₃ and Fe₂O₃ owing to amphoteric oxide, can be dissociated into MeO₄⁵⁻ or Me³⁺ ions in the melting state [17]. As shown in the following formulae:



Al (with an ionic radius of 0.57 Å) tends to form a tetrahedral MeO₄⁵⁻ ion, and Fe (with an ionic radius of 0.67 Å) tends to form an octahedral Me³⁺ ion. The tetrahedral valence bond of Me–O is strong and increases the viscosity of liquid phase, which is difficult to be

broken in the viscous flow. However, the valence bond of Me–O in octahedron is weak, and decreases the viscosity of liquid phase. Hence, composition and content of ferrite are the noteworthy concern for the formation of C_4A_3S and C_3S .

In this work, the composition of ferrite phase is general variation by adjusting the proportional between Fe_2O_3 and Al_2O_3 in raw mixes, where ferrite content is designed as 5 %, 10 %, 15 % and 20 %, respectively. The intention is to achieve the formation and coexistence of C_4A_3S and C_3S by changing the viscosity and the formation temperature of liquid phase. The coexistence of two minerals is beneficial for durative development of strength in clinker. It will be also beneficial to saving energy and reducing emission from manufacture.

EXPERIMENTAL

Sample preparation

In order to eliminate the effect of other impurities, analytical-grade $CaCO_3$, SiO_2 , $Al(OH)_3$, Fe_2O_3 and $CaSO_4 \cdot 2H_2O$ were used to synthesize the cement clinker. The prepared raw meals were homogenized in a ball mill bottle with agate balls for 4 h. The raw meals were mixed with water and pressed under a pressure of 16 MPa into a disk with $\Phi 45 \times 3$ mm. The dried disks were sintered in a resistance furnace at different temperatures (1320, 1350, 1380 and 1410°C) for 60 min. Subsequently, the cement clinker was removed from the furnace immediately and cooled rapidly by a fan. The theoretic mineral composition of the clinker was listed in Table 1. Choosing orthogonal list L16 (4^3), (L-orthogonal experiment, 16 experiments, 3 factors, and 4 tiers), as experiment regulation, was listed in Table 2.

Table 1. Theoretic mineral composition of the samples w (%).

C_3S^a	Clinker composition		
	C_2S	C_4A_3S	$C_2A_{1-X}F_X^b$
15	57	23	5
15	52	23	10
15	47	23	15
15	42	23	20

^a Notation: C = CaO, S = SiO_2 , A = Al_2O_3 , F = Fe_2O_3 , S = SO_3

^b X stands for the molar of Fe_2O_3 and can vary from 0.25 to 1 (X = 0.25, 0.5, 0.75 and 1)

Table 2. Factors and levels of orthogonal experiment.

Levels	Factor A	Factor B	Factor C
	The molar ratio of A/Fc	Burning temperature (°C)	Ferrite phase content (%)
1	3	1320	5
2	1	1350	10
3	1/3	1380	15
4	0	1410	20

^c A/F = Al_2O_3/Fe_2O_3

Characterization

Free lime tests

The content of free lime (f-CaO) in clinker was estimated using alcohol-glycerin method.

X-ray diffraction (XRD)

All clinker samples were ground into fine powder to perform laboratory X-ray powder diffraction studies. XRD data were collected on a Bruker AXS D8-Advance diffractometer with Cu K α radiation generated at 35 kV and 45 mA at room temperature. The powders were step scanned from 5° to 60° with a step size and time per step of 0.02° and 0.5 s, respectively.

Differential scanning calorimetry-thermogravimetric analysis

Thermal analysis was monitored on a Mettler-1600 HT instrument with a combined TG and DSC system. A portion of the raw materials powder was heated from 25°C to 1400°C at a heating rate of 10°C·min⁻¹ under air atmosphere.

Scanning electron microscopy analysis

SEM imaging using backscattered electrons requires a polished specimen for optimum performance [18]. The clinker sample was embedded and polished. After polishing, the clinker sample was cleaned using a clean polishing cloth. The final polished cross-sections were covered with carbon to provide a conductive surface for SEM imaging. Observation of mineral morphological feature, in particular C_4A_3S and C_3S minerals, was carried out on a scanning electron microscope (SEM, S4800, Hitachi). The element distributions of clinker minerals were evaluated by energy dispersive spectra analysis (EDS).

RESULTS AND DISCUSSION

The burnability of cement clinker

The content of f-CaO in clinker is a good indicator of the burning degree [19]. The f-CaO content of clinker samples with the amount of ferrite phase at different temperatures are presented in Figure 1. As the sintering temperatures and the F/A molar ratio increased, the content of f-CaO in clinker obviously decreases, and the trend is more obvious when Fe_2O_3 proportion ranges from 0.5 to 1. Moreover, the increase in ferrite content can promote the absorption of f-CaO at a relatively low temperature. The effect of Fe_2O_3 on the f-CaO content is attributed to the decrease in the formation temperature of liquid phase, which corresponds to the analysis of DTG-DSC measurement in later part of this paper.

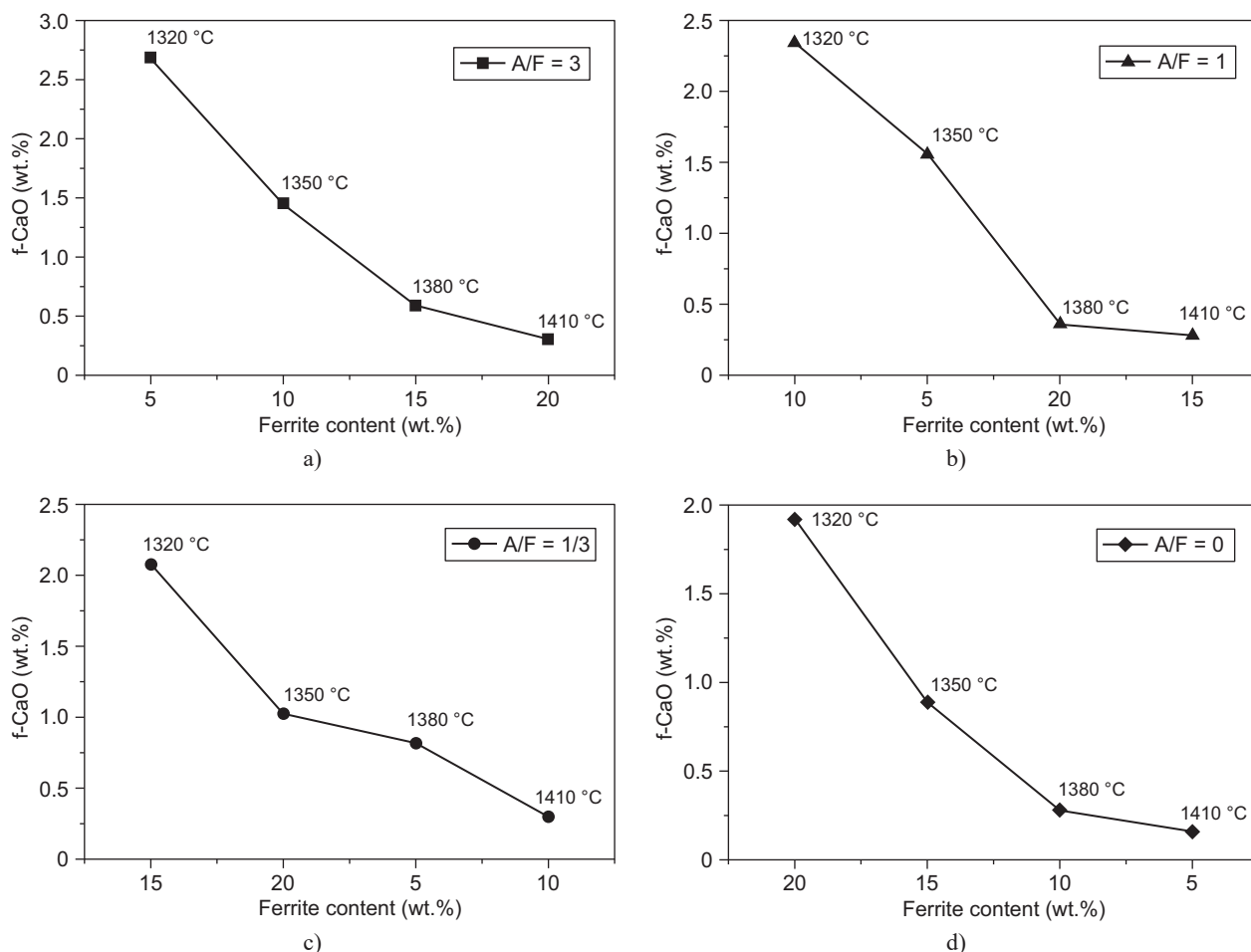


Figure 1. The effect of ferrite phase on free lime content in clinkers.

Burnability index (BI) also reveals the burnability of raw meals [20]. BI value can be calculated with contents of f-CaO in the clinker samples burnt at different temperatures from the formula: (3)

$$BI = 3.75 \frac{(A + B + 2C + 3D)}{\sqrt[4]{A - D}} \quad (3)$$

where A, B, C and D are the content of f-CaO in the clinkers calcined at 1320, 1350, 1380 and 1410 °C [21]. The low value of BI implies a good burnability. The clinker samples with good burnability are with BI value lower and equal to 60 [20]. BI values with the different compositions of ferrite phase is shown in Figure 2. With the F/A molar ratio increased, BI values of clinker samples generally decrease from 18.86 to 12.53. This results indicate that high amount of Fe_2O_3 can enhance the absorption of f-CaO, improve the burnability of clinker and accelerate the C_3S formation in the clinker.

The phase analysis of the cement clinker

XRD is used to analyze the phase composition of clinker samples. The XRD patterns of clinkers with the different composition and content of ferrite phase are

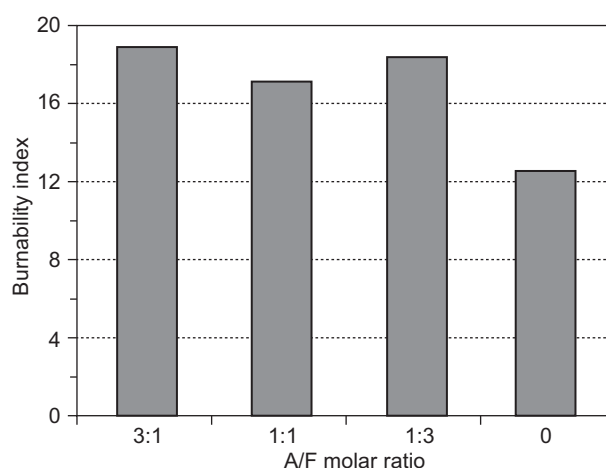


Figure 2. The effect of ferrite phase on the burnability index in clinkers.

shown in Figure 3. The clinker samples were burned at 1320, 1350, 1380 and 1410 °C. From Figure 3a, the clinker samples at different temperatures show similar mineral compositions. The clinker minerals are C_2S , $\text{C}_4\text{A}_3\text{S}$, C_3S and $\text{C}_2\text{A}_{0.5}\text{F}_{0.5}$ solid solutions by analysis of Jade software. When the content of ferrite is 20 %

at 1320°C, the diffraction peak of $C_4A_3\$$ is lower than other samples. It might be due to the fact that the actual composition of ferrite is $C_2A_{0.5}F_{0.5}$ (brownmillerite, $2\theta = 12.16^\circ$, $d = 7.27 \text{ \AA}$). Hence, more Al_2O_3 , which is used to generate $C_4A_3\$$, is consumed and forms brownmillerite in burning process. The diffraction peak of C_3S ($2\theta = 29.38^\circ$, $d = 3.03 \text{ \AA}$) is obviously high when the temperature reach to 1380°C and 1410°C, respectively. This result is consistent with the observations of SEM in later part of this paper.

The XRD patterns of the clinker samples with the A/F molar ratio of 1/3 are shown in Figure 3b. Likewise, clinker samples mainly consist of C_2S , $C_4A_3\$$, C_3S and $C_2A_{0.5}F_{0.5}$ solid solutions. The intensity of $C_4A_3\$$ peaks slightly increase in Figure 3b compared to Figure 3a. There is a relatively much Al_2O_3 being used to $C_4A_3\$$ crystal owing to increasing of A/F molar ratio in the raw mixtures. When the content of ferrite is 20 % at 1350°C, the diffraction peaks of $C_4A_3\$$ and C_3S are

remarkably high compared to the other clinker sample. The result illustrates that the quantity of liquid phase and its viscosity can promote the formation of C_3S , which further indicates that the A/F molar ratio with the composition of ferrite phases is important in the formation of clinker mineral. It is also in agreement with the SEM-EDS analysis. When the burning temperature is more than 1350°C, the intensity of $C_4A_3\$$ peaks obviously decreases. This suggests that $C_4A_3\$$ has already decomposed when the temperature is higher than its decomposition temperature. The sulfate in liquid phase generated by $C_4A_3\$$ decomposition inhibits the reaction of CaO with belite, consequently suppressing the C_3S formation [22-24]. Therefore, excessive the burning temperature does not facilitate the coexistence of $C_4A_3\$$ and C_3S .

The XRD patterns of the clinker samples with the A/F molar ratio of 1 are shown in Figure 3c. The clinker samples of different temperatures present similar

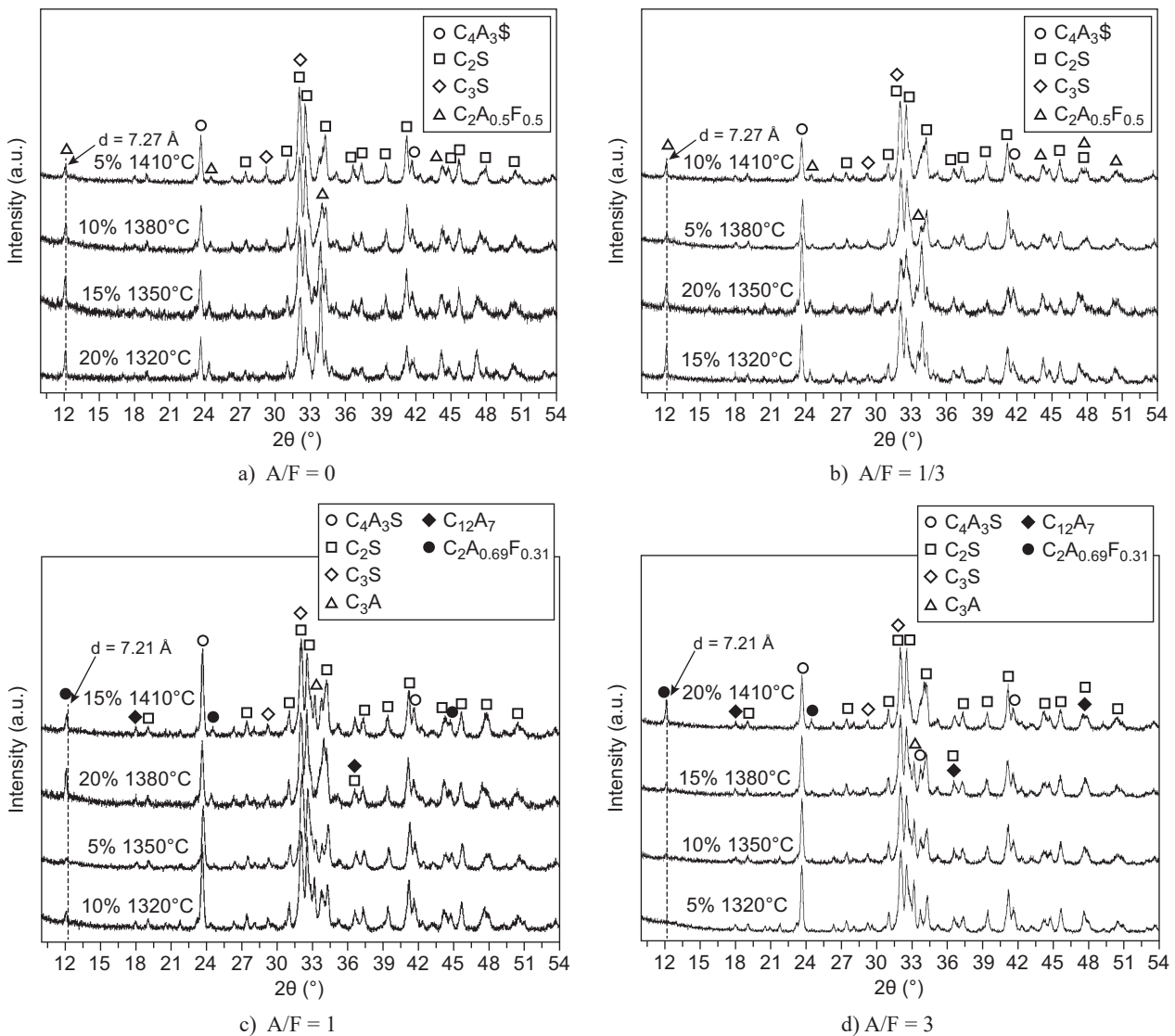


Figure 3. The XRD patterns of samples with different ferrite phases.

mineral compositions, all of them are C_2S , $\text{C}_4\text{A}_3\text{S}$, C_3S , C_3A , C_{12}A_7 and $\text{C}_2\text{A}_{0.69}\text{F}_{0.31}$ solid solutions by analysis of Jade software. When the molar ratio of A/F increases in raw mixes, the composition of ferrite phase is $\text{C}_2\text{A}_{0.69}\text{F}_{0.31}$ solid solution ($2\theta = 12.26^\circ$, $d = 7.21 \text{ \AA}$) in clinker samples. The main peak of $\text{C}_2\text{A}_{0.69}\text{F}_{0.31}$ shift to right higher angle compared with $\text{C}_2\text{A}_{0.5}\text{F}_{0.5}$. It might be due to the fact that C_2F itself contains iron as Fe^{3+} in both tetrahedral and octahedral sites, the latter being twice as numerous as the former. As Al is added to C_2F , it has smaller ionic radius than Fe and preferentially enters tetrahedral sites. Hence, the lattice parameters and the main reflection lines of the ferrite phase also move towards lower d-spacings (from 7.27 \AA to 7.21 \AA) with increasing Al_2O_3 content of the samples [25]. In addition, the characteristic diffraction peak of C_{12}A_7 ($2\theta = 18.03^\circ$) can be observed in Figures 3c and 3d, which means changing the composition of clinker samples by excessive consumption of CaO and Al_2O_3 in the burning process. Moreover, the diffraction peak of C_3A ($2\theta = 33.3^\circ$) in clinker samples is more visible apart from the content of ferrite phase in 20%. The result illustrates that the decomposition of $\text{C}_4\text{A}_3\text{S}$ can be facilitated with increasing Al_2O_3 content of the raw mixes in burning process, and then inhibiting the C_3S formation. Furthermore, flash setting mineral C_{12}A_7 and C_3A are not normally found in clinker samples. This adversely influences the quality of cement, decreasing the fluidity and increasing the heat of hydration [26].

From Figure 3d, the clinker samples with the A/F molar ratio of 3 at different temperatures present similar mineral compositions, all of them are C_2S , $\text{C}_4\text{A}_3\text{S}$, C_3S , C_3A , C_{12}A_7 and $\text{C}_2\text{A}_{0.69}\text{F}_{0.31}$ solid solutions. The diffraction peak of $\text{C}_4\text{A}_3\text{S}$ is generally weakened and the characteristic peak of C_3S are almost not observed with the increasing burning temperatures. It is probably related to the decomposition of $\text{C}_4\text{A}_3\text{S}$ at temperature higher than 1350°C [27, 28] which provides an unfavorable condition for the formation of C_3S . In general, the intensity of diffractive peak is related to the content and crystallinity of phase [29]. Therefore, this suggests that excessive the A/F molar ratio not facilitates the formation of C_3S and the coexistence of $\text{C}_4\text{A}_3\text{S}$ and C_3S . Thus, it can be drawn that the composition and content of liquid phase have the significantly effect on the formation of clinker mineral.

Thermal analysis

The thermal analysis curves of raw mixes at different ferrite phases are given in Figure 4. The results carried out the raw mixes are used to obtain information on the decomposition and the formation of chemical compounds during burning process. The first endothermic peak about 120°C is attributed to the decomposition of gypsum in the raw mixtures. The second endothermic peak located at approximately 285°C is proven to be the decomposition

of $\text{Al}(\text{OH})_3$ [13, 30]. The third peak between 650°C and 850°C is attributed to the decomposition of CaCO_3 . The fourth peak at approximately 1230°C is ascribed to the formation of liquid phase and C_3S mineral. When the content of ferrite phase is the same with 15% in raw mixes, but its composition is different, the decomposition temperature of CaCO_3 in samples with A/F molar ratio of 3 and 0 are 830.3°C and 834.4°C , respectively, implying that the composition of ferrite phase has a slight influence on the decomposition temperature of CaCO_3 . However, the formation of liquid phase and C_3S is strongly affected by the composition of ferrite phase. The formation temperatures of liquid phase in raw mixes with 15% content of ferrite phase are about 1190.9°C and 1237.1°C , respectively. The result further illustrates that the decrease of A/F molar ratio can lower the formation temperature of liquid phase. At the same time, it provides a favorable condition for the formation of C_3S in burning process, which is consistent with previous results of XRD observations.

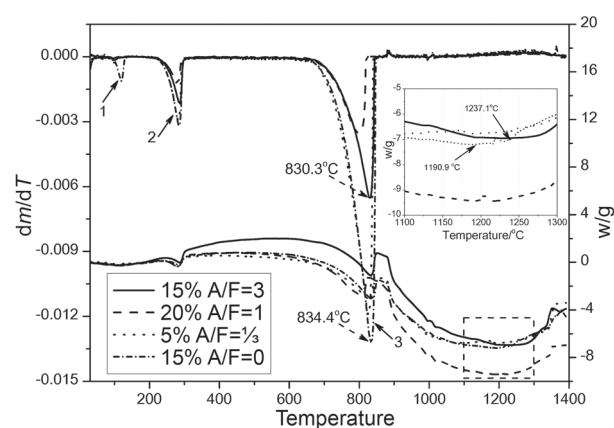


Figure 4. DTG-DSC curves of raw materials at different ferrite phases.

SEM-EDS analysis

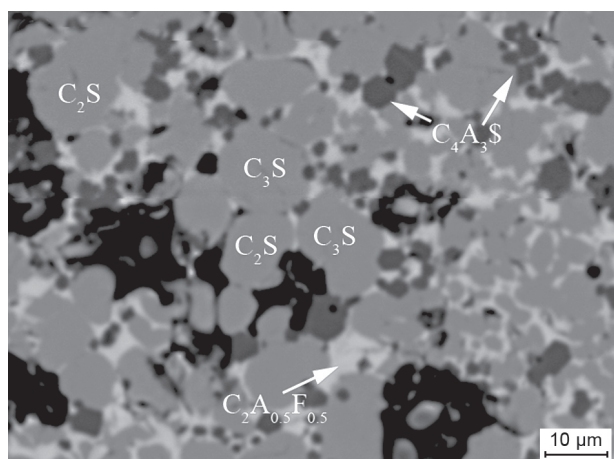
The morphological feature of clinker minerals was observed by BSE and EDS with area scanning map to determine the distribution of clinker minerals in Figure 5. The microstructure changes markedly with different A/F molar ratio and the sintering temperature. However, the microstructure revealed the formation of solid solutions inside the equilibrium phase assemblage all samples, namely, C_2S , $\text{C}_4\text{A}_3\text{S}$, C_3S and $\text{C}_2\text{A}_{0.5}\text{F}_{0.5}$ solid solutions. Microstructure of the clinker sample is loose at a relatively low burning temperature (1350°C) from Figure 5a. Most of the silicate phases are C_2S , and C_3S solid solution is rarely, as corroborated by the XRD analysis. The dark grains are $\text{C}_4\text{A}_3\text{S}$ solid solutions, and their sizes are approximate $10 \mu\text{m}$. Their outlines are also the distinct polygon in the clinker sample. The large bright and reflective crystals which partially surround the

C_4A_3S crystals are ferrite. The result indicates that C_4A_3S crystals have not dissolved in liquid phase at 1350°C and retains regular outlines with undercooling, which also coincide well with XRD results.

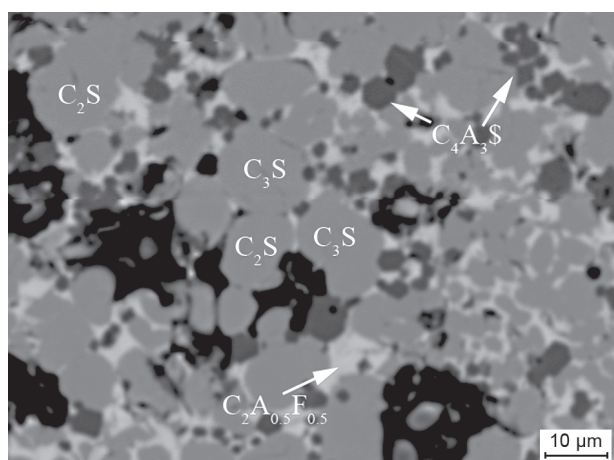
Compared with C_4A_3S grains at the burning temperature 1350°C (Figure 5a), the sample with the molar ratio A/F as 0 at 1380°C is smaller than $10\ \mu\text{m}$, as shown in Figure 5b, and its outline is unclear. This result suggests that a part of C_4A_3S has decomposed in the liquid phase and formed the solid solution with silicate phase, which also is consistent well with the molar ratio of element from EDS analysis [31]. In contrast, the C_2S and C_3S crystal have larger particle sizes more than $10\ \mu\text{m}$, and the sample in Figure 5b has a lower porosity

Point +2 element	Molar ratio	Point +1 element	Molar ratio
Ca	24.33	Ca	41.02
Al	23.35	Si	11.47
O	44.07	O	42.52
S	4.43	Al	3.54
Fe	1.60	Fe	0.68
Si	2.23	S	0.77

a) with 20 % ferrite phase (A/F = 1/3)



b) with 10 % ferrite phase (A/F = 0)



c) with 5 % ferrite phase (A/F = 0)

Figure 5. BSE image of samples with different ferrite phases.

because the increasing amount of liquid at 1380°C can promote the formation of C_3S . With the ongoing increase in the burning temperature, the clinker sample shows well-formed hexagon C_3S crystals and large circular C_2S crystals, which are encompassed by ferrite phases. However, accompanied by the decomposition of C_4A_3S , its crystal size becomes small only several microns from Figure 5c. This has an adverse effect on the coexistence of C_4A_3S and C_3S crystals. Hence, it must be remembered that the ferrite phase plays an important role in avoiding the breakdown of C_4A_3S and facilitating the formation of C_3S in the sintering process.

CONCLUSIONS

In order to achieve the coexistence of C_3S and C_4A_3S , the effect of ferrite phase on the formation and coexistence of two clinker minerals was investigated by changing the A/F molar ratio. The following conclusions can be drawn from this study:

- When the composition of ferrite is $C_2A_{0.5}F_{0.5}$ with the A/F molar ratio of 1/3 and its content is 20 % at 1350°C , the property of liquid phase can facilitate the coexistence of C_4A_3S and C_3S solid solutions. However, it has an adverse effect on the coexistence of two clinker minerals with the increasing the A/F molar ratio, meanwhile, the formation of $C_{12}A_7$ and C_3A has a negative effect on the setting times of clinkers.
- Ferrite phase of the decreasing A/F molar ratio can significantly lower the formation temperature of liquid phase. Consequently, it can facilitate the burnability of the raw mixes and provide a favorable condition for the formation of C_3S in burning process.
- The distinctly dark and polygonal C_4A_3S solid solutions, whose sizes are approximate $10\ \mu\text{m}$, has not dissolved in liquid phase at 1350°C . However, with the increase of the sintering temperature, a part of C_4A_3S has decomposed in the liquid phase and formed the solid solution, and its crystal size becomes smaller and its outlines is also unclear.

Acknowledgements

The authors are grateful for the financial support of the National Key Research and Development Program (2016YFB0303505) and the National Natural Science Foundation of China (Grant No.51272092).

REFERENCES

1. Taylor H. F. W. (1990). *Cement chemistry*. Thomas Telford Publishing, London.
2. Janotka I., Krajčí L. Ě. (2000): Resistance to freezing and thawing of mortar specimens made from sulphoaluminate-belite cement. *Bulletin of Materials Science*, 23 (6),

- 521-527. doi:10.1007/BF02903894
3. Álvarez-Ayuso E., Querol X., Tomás A. (2006): Environmental impact of a coal combustion-desulphurisation plant: Abatement capacity of desulphurisation process and environmental characterisation of combustion byproducts. *Chemosphere*, 65 (11), 2009-2017. doi:10.1016/j.chemosphere.2006.06.070
 4. Odler I., Zhang H. (1996): Investigations on high SO_3 portland clinkers and cements I. Clinker synthesis and cement preparation. *Cement and Concrete Research*, 26 (9), 1307-1313. doi:10.1016/0008-8846(96)00128-7
 5. Zhang H., Odler I. (1996): Investigations on high SO_3 Portland clinkers and cements II. Properties of cements. *Cement and Concrete Research*, 26 (9), 1315-1324. doi:10.1016/0008-8846(96)00129-9
 6. Liu X., Li Y., Zhang N. (2002): Influence of MgO on the formation of Ca_3SiO_5 and $3\text{CaO}\cdot 3\text{Al}_2\text{O}_3\cdot \text{CaSO}_4$ minerals in alite sulphoaluminate cement. *Cement and Concrete Research*, 32 (7), 1125-1129. doi:10.1016/S0008-8846(02)00751-2
 7. Liu X., Li Y. (2005): Effect of MgO on the composition and properties of alite-sulphoaluminate cement. *Cement and Concrete Research*, 35 (9), 1125-1129. doi:10.1016/j.cemconres.2004.08.008
 8. Ma S., Shen X., Gong X., Zhong B. (2006): Influence of CuO on the formation and coexistence of $3\text{CaO}\cdot \text{SiO}_2$ and $3\text{CaO}\cdot 3\text{Al}_2\text{O}_3\cdot \text{CaSO}_4$ minerals. *Cement and Concrete Research*, 36 (9), 1784-1787. doi:10.1016/j.cemconres.2006.05.030
 9. Ma S., Snellings R., Li X. (2013): Alite-ye'elimite cement: Synthesis and mineralogical analysis. *Cement and Concrete Research*, 45, 15-20. doi:10.1016/j.cemconres.2012.10.020
 10. Shen X., Ma S., Li X. (2013). *Secondary synthetic method for calcium sulphoaluminate mineral in Portland cement clinker*. US8404039B2.
 11. Chitvoranund N., Sinthupinyo S., Winnefeld F., Lothenbach B. (2017): Synthesis and hydration of alite-calcium sulfoaluminate cement. *Advances in Cement Research*, 29, 101-111. doi:10.1680/jadcr.16.00071
 12. Duvallet T. Y. F. (2014). *Influence of Ferrite Phase in Alite-Calcium Sulfoaluminate Cements*, PhD thesis, University of Kentucky, Lexington, KY, USA.
 13. Londono-Zuluaga D., Tobon J.I., Aranda M.A.G. (2017): Clinkering and hydration of belite-alite-ye'elimite cement. *Cement and Concrete Composites*, 80, 333-341. doi:10.1016/j.cemconcomp.2017.04.002
 14. Herfort D., Moir G. K., Johansen V., Sorrentino F., Arceo H. B. (2010): The chemistry of Portland cement clinker. *Advances in Cement Research*, 22 (4), 187-194. doi:10.1680/adcr.2010.22.4.187
 15. Yang J., Li W., Li Z., et al. (2013): *Flame-resistant corrosion-resistant coating*. CN102815951A.
 16. Kacimi L., Simon-Masseron A., Ghomari A., Derriche Z. (2006): Influence of NaF, KF and CaF_2 addition on the clinker burning temperature and its properties. *C. R. Chimie*, 9, 154-163. doi:10.1016/j.crci.2005.10.001
 17. Shen W., Min P., Huang W. (2005). *Cement Technology*. Wuhan University of Technology Press, Wuhan.
 18. Stutzman P.E., Clifton J.R. (1999). Speciment preparation for scanning electron microscopy, in: L. Jany, A. Nisperos (eds.), *Proceedings of the Twenty-First International Conference on Cement Microscopy*, International Cement Microscopy Association, pp.10-22.
 19. Stephan D., Mallmann R., Knöfel D., Härdtl R. (1999): High intakes of Cr, Ni, and Zn in clinker: Part I. Influence on burning process and formation of phases. *Cement and Concrete Research*, 29 (12), 1949-1957. doi:10.1016/S0008-8846(99)00195-7
 20. Ifka T., Palou M.T., Bazelová Z. (2012): The influence of CaO and P_2O_5 of bone ash upon the reactivity and the burnability of cement raw mixtures. *Ceramics-Silikáty*, 56 (1), 76-84.
 21. Marroccoli M., Montagnaro F., Pace M.L., Telesca A., Valenti G.L. (2009). Coal Combustion Ash as a Raw Mix Component for Portland Cement Manufacture, in: *32nd Meeting on Combustion*, Combustion Colloquia, pp. V2(1)-V2(5).
 22. Horkoss S, Lteif R, Rizk T. (2011): Influence of the clinker SO_3 on the cement characteristics. *Cement & Concrete Research*, 41 (8), 913-919. doi:10.1016/j.cemconres.2011.04.015
 23. Taylor H. F. W. (1999): Distribution of sulfate between phases in Portland cement clinkers. *Cement and Concrete Research*, 29 (8), 1173-1179. doi:10.1016/S0008-8846(98)00241-5
 24. Strunge J, Knoefel D, Dreizler I. (1985): Effect of alkalis and sulfur on the properties of cement Part I. Effect of the sulfur trioxide content on cement properties. *Zement-Kalk-Gips Ed. B.* 38, 150-158.
 25. Hewlett P. (2004). *Lea's Chemistry of Cement and Concrete*, 4th ed. Elsevier Science & Technology Books Publishing, Amsterdam.
 26. Kurokawa D., Honma K., Hirao H., Fukuda K. (2013): Quality design of belite-melilite clinker. *Cement and Concrete Research*, 54, 126-132. doi:10.1016/j.cemconres.2013.09.004
 27. Juenger M. C. G., Winnefeld F., Provis J. L., Ideker J. H. (2011): Advances in alternative cementitious binders. *Cement and Concrete Research*, 41 (12), 1232-1243. doi:10.1016/j.cemconres.2010.11.012
 28. Snellings R., De Schepper M., De Buysser K., Driessche I., Belie N (2012): Clinkering reactions during firing of recyclable concrete. *Journal of the American Ceramic Society*, 95, 1741-1749. Doi: 10.1111/j.1551-2916.2012.05168.x
 29. Shang D., Wang M., Xia Z. (2017): Incorporation mechanism of titanium in Portland cement clinker and its effects on hydration properties. *Construction and Building Materials*, 146, 344-349. doi:10.1016/j.conbuildmat.2017.03.129
 30. Chang J., Zhang Y., Shang X., Zhao J., Yu X. (2017): Effects of amorphous AH_3 phase on mechanical properties and hydration process of $\text{C}_4\text{A}_3\text{S}-\text{CSH}_2-\text{CH}-\text{H}_2\text{O}$ system. *Construction and Building Materials*, 133, 314-322. doi:10.1016/j.conbuildmat.2016.11.111
 31. Strigác J., Palou M. T., Kristin J., Majling J. (2000): Morphology and chemical composition of minerals inside the phase assemblage $\text{C}-\text{C}_2\text{S}-\text{C}_4\text{A}_3\text{S}-\text{C}_4\text{AF}-\text{CS}$ relevant to sulfoaluminate belite cements. *Ceramics-Silikáty*, 44, 26-34.